The Journal of Experimental Biology 205, 3281–3298 (2002)
Printed in Great Britain © The Company of Biologists Limited
JEB4256

Does reflection polarization by plants influence colour perception in insects? Polarimetric measurements applied to a polarization-sensitive model retina of *Papilio* butterflies

Gábor Horváth[1,*], József Gál[2], Thomas Labhart[3] and Rüdiger Wehner[3]

[1]*Biooptics Laboratory, Department of Biological Physics, Eötvös University, H-1117 Budapest, Pázmány sétány 1, Hungary,* [2]*International University Bremen, School of Engineering and Science, P.O.B. 750561, D-28725 Bremen-Grohn, Campus Ring 1, Germany* and [3]*Institut für Zoologie, Universität Zürich, CH-8057 Zürich, Winterthurerstrasse 190, Switzerland*

*Author for correspondence (e-mail: gh@arago.elte.hu)

Accepted 6 August 2002

Summary

Using imaging polarimetry, we have measured some typical reflection-polarization patterns of plant surfaces (leaves and flowers) under different illuminations. Using a quantitative model to determine photon absorptions in the weakly polarization-sensitive (*PS*≈2) photoreceptors of *Papilio* butterflies, we have calculated the influence of reflection polarization on the colours of leaves and flowers perceived by *Papilio*. Compared with a retina containing polarization-blind colour receptors, the colour loci of specularly reflecting and, thus, strongly polarizing areas on a plant are slightly shifted, which could cause the perception of false colours. However, the colour of specularly reflecting surfaces is strongly masked by white glare, which may prevent the perception of polarization-induced hue shifts. Although the perception of polarizational false colours by *Papilio* butterflies was previously demonstrated with artificial, strongly colour-saturated and totally linearly polarized stimuli, we expect that the weak polarization sensitivity of *Papilio* photoreceptors hardly influences colour perception under natural conditions.

Key words: polarization sensitivity, colour perception, polarizational false colours, reflection polarization, imaging polarimetry, computer modelling, plant–insect interactions.

Introduction

As was demonstrated by Karl von Frisch (1965), honeybees (*Apis mellifera*) respond to skylight polarization and use it for navigation. The ultraviolet- (UV) and polarization-sensitive photoreceptors concerned are gathered in an upward-pointing narrow area of the eye, the so-called 'POL area' (Wehner and Strasser, 1985). Except for this specialized polarization-sensitive channel, the retina of honeybees is composed of photoreceptors that are twisted about their longitudinal axes (Wehner et al., 1975), so that their polarization sensitivity is almost abolished (Labhart, 1980). Similar twisted photoreceptors, or receptors in which the microvilli of the rhabdomeres are not aligned consistently in a single particular direction, have also been found in desert ants (*Cataglyphis bicolor*), flies (*Calliphora erythrocephala*), crickets (*Gryllus campestris*) and beetles (*Melolontha melolontha*) (see Wehner and Bernard, 1993). In these photoreceptors, the polarization sensitivity is weak, whereas the straight (untwisted) receptors located at the dorsal rim of the eye and used exclusively for detecting polarized skylight exhibit high polarization sensitivity [for example, in bees, the polarization sensitivity (*PS* value) of ultraviolet receptors ranges from 5 to 18 (Labhart, 1980)].

Wehner and Bernard (1993) proposed that the functional significance of the photoreceptor twist is to avoid the polarization-induced false colours of natural, bee-relevant surfaces such as leaves and petals of flowers, which reflect partially linearly polarized light. The degree and angle of polarization of reflected light depend on how smooth the plant surfaces are and how they are oriented with respect to the incoming light at the direction of view. For a flower-visitor, this could cause difficulties, because the absorbing photopigments responsible for colour vision are contained in receptors with different microvillar orientations. Thus, each receptor gives a signal that depends not only on intensity and wavelength but also on the angle and degree of polarization. If the sensors of a colour vision system are also polarization sensitive, the system generates 'false colours' that may obscure the real colours defined by the spectral properties of the object.

Recently, Kelber (1999a) and Kelber et al. (2001) suggested that the butterflies *Papilio aegeus* and *Papilio xuthus* do not process polarization and colour separately, and thus they may perceive polarization-induced false colours

owing to their weakly polarization-sensitive photoreceptors. As Kelber and collaborators worked with artificial stimuli that had an unnaturally high degree of linear polarization (100%; i.e. totally polarized light, which is not characteristic of light reflected from plant surfaces), no published behavioural data so far support that there is a significant influence of polarization on butterfly colour vision under natural conditions, when the receptors are stimulated by partially linearly polarized light with frequently low degrees of polarization.

As the *PS* value of photoreceptors in *Papilio* species, ranging between 1.3 and 2 (Bandai et al., 1992; Kelber et al., 2001), is very low (note that *PS*=1 for polarization-insensitive receptors), the following question arises: can the often low degree of polarization of light reflected from plant surfaces induce sufficiently strong polarizational false colours in *Papilio* butterflies to influence their colour vision significantly? How do these polarization-induced false colours depend on the different parameters of the butterfly retina (microvillar directions, polarization sensitivity or orientation of the eye), on the characteristics of the optical stimuli (degree and angle of polarization of reflected light) and on the illumination conditions (alignment of the plant surface with respect to the direction of view and to the solar direction; plant surface in direct sunshine and in shadow).

In the present study, we have quantitatively estimated the influence of polarization sensitivity on the perception of natural surface colours by *Papilio* butterflies. We measured the characteristics of polarized light reflected from plant surfaces by imaging polarimetry (Horváth and Varjú, 1997) in the field under natural illumination conditions. Recently, Shashar et al. (1998) demonstrated some features of polarized light reflected from leaves in a tropical rain forest. The first aim of our work is to present some typical reflection-polarization patterns of plants (flowers and leaves). The second aim is to give a quantitative model to calculate the quantum flux absorbed by polarization-sensitive photoreceptors of *Papilio* butterflies from the measured polarization patterns and to calculate the loci of the perceived false colours in the colour triangle of their simplified colour vision system. We investigated the influence of the microvillar direction, polarization sensitivity, orientation of the eye, degree and angle of polarization of reflected light, alignment of the plant surface with respect to the direction of view, and the solar direction on the polarization-induced false colours perceived by *Papilio* butterflies. We also studied how the polarizational false colours differ under direct sunlight and in the shade. Finally, we discuss the limitations of our polarimetric technique and computer modelling.

Materials and methods

Imaging polarimetric measurement of reflection-polarization characteristics of plant surfaces

As an imaging polarimeter, we used a professional 3CCD-VX1E Sony Hi8 video camera (possessing three separate CCD detectors for the blue, green and red ranges of the spectrum) mounted with a neutral density (grey) rotatable linearly polarizing filter (Hama) in front of the objective lens. The three CCD chips of the camera are maximally sensitive at wavelengths λ_B^c=450 nm (blue), λ_G^c=550 nm (green) and λ_R^c=650 nm (red), with half bandwidths of approximately 80 nm (data supplied by the manufacturer). The spatial distribution of the intensity *I*, the degree of linear polarization δ and the angle of polarization χ (with respect to the vertical) of different plant surfaces were measured by video polarimetry at these three wavelengths. The method is described in detail by Horváth and Varjú (1997).

Computation of the spectral loci of colours perceived by a polarization- and colour-sensitive retina

The numerical values of our retina model (Fig. 1A,B) described in this subsection are characteristic of the butterfly *Papilio xuthus* L. (fig. 1B and table 1 of Kelber et al., 2001, pp. 2470-2471). Our model retina contains polarization-sensitive photoreceptors of spectral types red (R), green (G) and blue (B), with the following sensitivity maxima: λ_R^r=600 nm, λ_G^r=520 nm and λ_B^r=460 nm, respectively. The relative absorption functions of the receptors are shown in Fig. 1A. In our retina model, angle β is the direction of the microvilli measured clockwise from the dorso-ventral meridian of the compound eye (Fig. 1C). For the microvilli of the blue-sensitive photoreceptors, β_B=0°, for the microvilli of the green-sensitive receptors β_G=0°, 35°, 90° or 145°, and for the microvilli of the red-sensitive receptors β_R=0°, 35° or 145° (Fig. 1B). The colour vision system of *Papilio* butterflies is pentachromatic (Arikawa et al., 1987). Treating the short-wavelength receptors (UV, violet, blue) as one receptor type allows us to demonstrate false-colour effects in a plausible way by indicating the shifts of colour loci in the equilateral colour triangle (Fig. 1E). No principally different false-colour effects are expected by including all five receptor types in our retina model. The soundness of this simplification is thoroughly discussed later in this article.

If the electric field vector (subsequently referred to as 'e-vector') of totally linearly polarized incident light is parallel (par) to the longitudinal axes of the microvilli, a polarization-sensitive photoreceptor of type *r* (=R,G,B) absorbs P_r times the number of photons (subsequently referred to as 'quantum absorption') as in the case when the e-vector is perpendicular (perp) to the microvilli. Thus, the relationship between the numbers of absorbed quanta (q) is: $q_r^{par}=P_r q_r^{perp}$, where P_r is the *PS* value of the receptor, and q_r is the quantum absorption. The polarization sensitivity of the photoreceptors in *P. xuthus* ranges from 1.3 to 2.0 at peak wavelengths (Kelber et al., 2001, p. 2471; table 1). In our retina model, we chose $P_B=P_G=P_R=2$, by which the average polarization sensitivity was slightly overestimated.

Let the angle of the eye's dorso-ventral meridian be α°

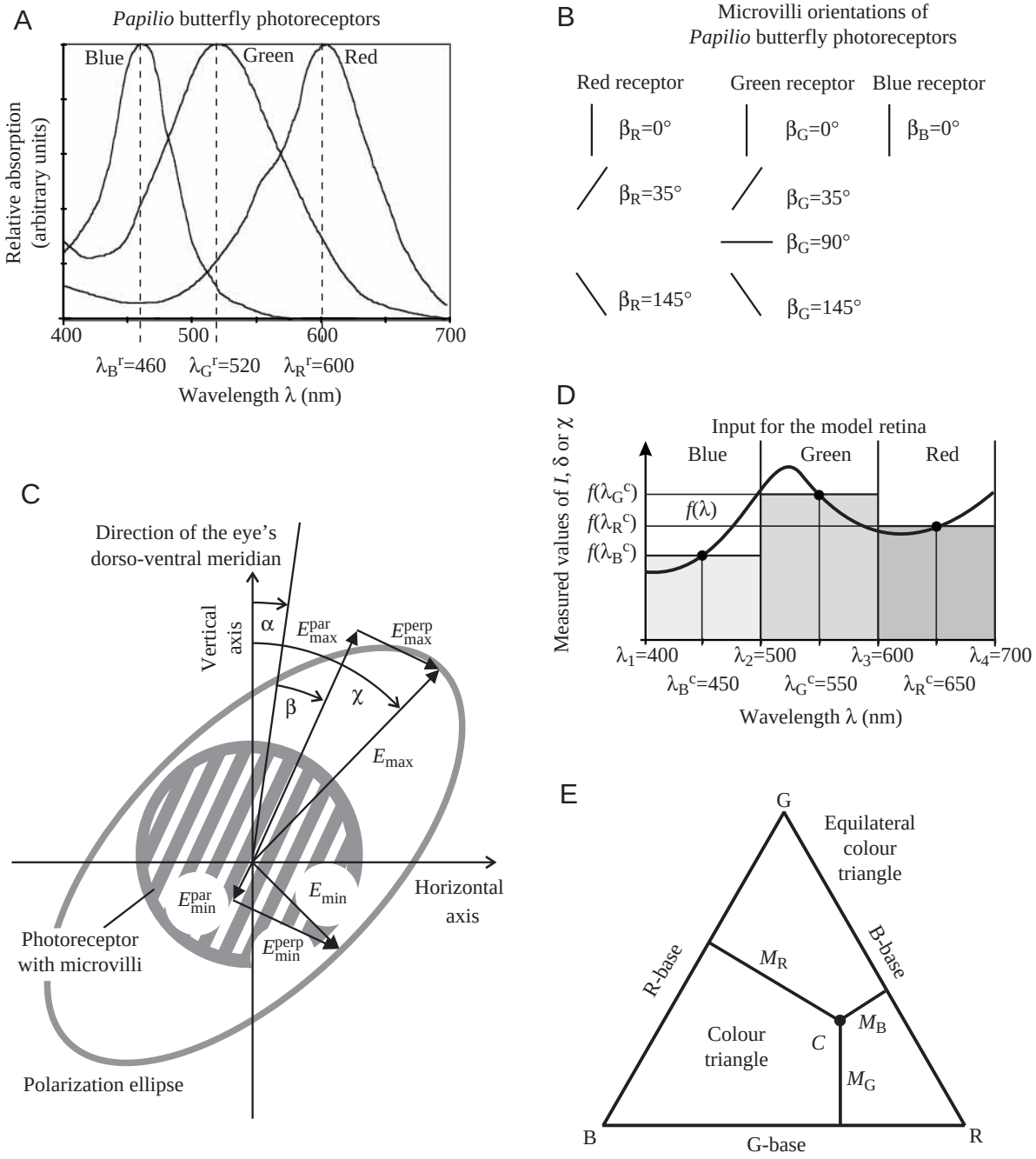

Fig. 1. (A) Relative absorption functions of the blue-, green- and red-sensitive receptors of the butterfly *Papilio xuthus* (Kelber et al., 2001). (B) Microvilli orientations (β) measured clockwise from the eye's dorso-ventral meridian in the photoreceptors of different spectral types (red, green and blue) in *P. xuthus* (Kelber et al., 2001). (C) Definition of the different parameters of partially linearly polarized light and a polarization-sensitive photoreceptor. The hatched area indicates the microvilli orientation β. The angle of the eye's dorso-ventral meridian is α clockwise from the vertical. χ is the angle of polarization of light measured clockwise from the vertical. The arrows represent the maximum (E_{max}) and minimum (E_{min}) electric field vectors (the major and minor axes of the polarization ellipse) and their components that are parallel (E_{min}^{par}, E_{max}^{par}) or perpendicular (E_{min}^{perp}, E_{max}^{perp}) to the microvilli. (D) Replacement of the blue (400–500 nm), green (500–600 nm) and red (600–700 nm) parts of function $f(\lambda)$ [$f=I$ (intensity) or $f=\delta$ (degree of linear polarization) or $f=\chi$ (angle of polarization)] by discrete constant values $f(\lambda_r^c)$ (*r* = blue, green, red) measured by video polarimetry at wavelengths λ_r^c. (E) Position of a visual stimulus *C* with spectral components M_R, M_G and M_B within the equilateral colour triangle of a colour-sensitive visual system with photoreceptor types R, G and B.

clockwise from the vertical (Fig. 1C). If receptor *r* receives partially linearly polarized light with intensity $I(\lambda)$, degree of linear polarization $\delta(\lambda)$, angle of polarization $\chi(\lambda)$ (clockwise from the vertical), minimum and maximum e-vectors $E_{min}(\lambda)$ and $E_{max}(\lambda)$, respectively, then q_r can be calculated as follows (Fig. 1C):

$$q_r = k \int_0^\infty A_r(\lambda)\Big[P_r E_{max}^{par}(\lambda)^2 + E_{max}^{perp}(\lambda)^2 + P_r E_{min}^{par}(\lambda)^2 + E_{min}^{perp}(\lambda)^2 \Big] d\lambda , \quad (1)$$

where k is a constant, λ is the wavelength of light, $A_r(\lambda)$ is the relative absorption of the receptor (Fig. 1A), $E_{max}^{par}(\lambda)$, $E_{max}^{perp}(\lambda)$ and $E_{min}^{par}(\lambda)$, $E_{min}^{perp}(\lambda)$ are the parallel and perpendicular components of the electric field vectors $E_{max}(\lambda)$ and $E_{min}(\lambda)$ with respect to the microvillar direction. From Fig. 1C, one can read:

$$\begin{aligned} E_{max}^{par}(\lambda) &= E_{max}(\lambda)\cos[\chi(\lambda) - \alpha - \beta_r] , \\ E_{max}^{perp}(\lambda) &= E_{max}(\lambda)\sin[\chi(\lambda) - \alpha - \beta_r] , \\ E_{min}^{par}(\lambda) &= -E_{min}(\lambda)\sin[\chi(\lambda) - \alpha - \beta_r] , \\ E_{min}^{perp}(\lambda) &= E_{min}(\lambda)\cos[\chi(\lambda) - \alpha - \beta_r] . \end{aligned} \quad (2)$$

The relationship between $E_{min}^2(\lambda)$, $E_{max}^2(\lambda)$ and $\delta(\lambda)$ is:

$$E_{min}^2(\lambda) = E_{max}^2(\lambda)[1 - \delta(\lambda)]/[1 + \delta(\lambda)] . \quad (3)$$

The intensity $I(\lambda)$ can be expressed with $E_{min}(\lambda)$ and $E_{max}(\lambda)$ as follows:

$$I(\lambda) = k'[E_{max}^2(\lambda) + E_{min}^2(\lambda)]/2 = k' E_{max}^2(\lambda)/[1 + \delta(\lambda)] , \quad (4)$$

where k′ is a constant. Using Equations 1–4, one obtains:

$$q_r = k'' \int_0^\infty A_r(\lambda) I(\lambda) \Big\{ P_r[1 + \delta(\lambda)] + 1 - \delta(\lambda) - 2\delta(\lambda)(P_r - 1)\sin^2[\chi(\lambda) - \alpha - \beta_r] \Big\} d\lambda , \quad (5)$$

where r = R,G,B, and k″ is a constant.

The expressions for k, k′ and k″ involve different electrodynamic constants. Using them, one could calculate the absolute value of q_r. We omit to give the expressions for k, k′ and k″ because they are all eliminated in the final expressions describing the spectral loci of colours perceived by a polarization- and colour-sensitive retina.

As we could measure the spatial distribution of intensity I, degree of polarization δ and angle of polarization χ of light reflected from plant surfaces only at wavelengths λ_B^c=450 nm, λ_G^c=550 nm and λ_R^c=650 nm, we took the following approximations in the calculation (Fig. 1D):

$$\begin{aligned} f(400\,\text{nm} \leqslant \lambda \leqslant 500\,\text{nm}) &= f(\lambda_B^c) = f_{blue} , \\ f(500\,\text{nm} < \lambda < 600\,\text{nm}) &= f(\lambda_G^c) = f_{green} , \\ f(600\,\text{nm} \leqslant \lambda \leqslant 700\,\text{nm}) &= f(\lambda_R^c) = f_{red} , \quad f = I, \delta, \chi ; \end{aligned} \quad (6)$$

in other words, in the spectral range s = red, green, blue, the values of I, δ and χ were considered to be constant. This approximation can be applied, because the maxima and half bandwidths of the red, green and blue sensitivity functions of the camera of our imaging polarimeter fall close to those of the corresponding red, green and blue relative absorption functions $A(\lambda)$ (Fig. 1A) of the butterfly retina modelled. Then:

$$q_r = k'' \sum_s I_s \Big[P_r(1 + \delta_s) + 1 - \delta_s - 2\delta_s(P_r - 1)\sin^2(\chi_s - \alpha - \beta_r) \Big] \int_{\lambda_{s1}}^{\lambda_{s2}} A_r(\lambda) d\lambda , \quad (7)$$

where r=R,G,B; s = red, green, blue; λ_{B1}=400 nm, λ_{B2}=λ_{G1}=500 nm, λ_{G2}=λ_{R1}=600 nm, and λ_{R2}=700 nm.

In the literature of colour vision, there are two different conventions to give the relative absorption functions $A(\lambda)$ of photoreceptors: they possess either equal amplitude $A_{max}(\lambda)$=1 (e.g. Przyrembel et al., 1995; fig. 12, p. 584) or equal integrals $\int_0^\infty A(\lambda)d\lambda$=1 (e.g. Lunau and Maier, 1995; fig. 1A, p. 3). Kelber et al. (2001), for example, used the first convention; our Fig. 1A gives the $A(\lambda)$ curves with the same amplitudes adapted from fig. 1B of Kelber et al. (2001). This convention is called ‘amplitude normalization’. The second convention, called ‘integral normalization’, corresponds to the assumption that the quantum absorptions of receptors of different spectral types are the same if the incident light is unpolarized [$\delta(\lambda)$=0] and physically white [$I(\lambda)$=constant]. This has the consequence that ‘physical (or optical) white’ coincides with ‘physiological (or perceptional) white’; in other words, the locus of both physical and physiological white is positioned at the colourless centre of the equilateral colour triangle of a trichromatic colour vision system (Fig. 1E). In this case, the receptor absorption curves are normalized by setting their integral to 1. In other words, the quantum absorption q_r of receptor type r is divided by the quantum absorption of the receptor for unpolarized (δ_s=0) and physically white light (I_s=I_{white} = arbitrary constant):

$$q_r^{white} = k'' I_{white}(P_r + 1) \sum_s \int_{\lambda_{s1}}^{\lambda_{s2}} A_r(\lambda) d\lambda . \quad (8)$$

Then, the normalized quantum absorption m_r is:

$$m_r = q_r / q_r^{white} = \Big\{ k'' \sum_s I_s \Big[P_r(1 + \delta_s) + 1 - \delta_s - 2\delta_s(P_r - 1)\sin^2(\chi_s - \alpha - \beta_r) \Big] \int_{\lambda_{s1}}^{\lambda_{s2}} A_r(\lambda) d\lambda \Big\} \Big/ \Big[k'' I_{white}(P_r + 1) \sum_s \int_{\lambda_{s1}}^{\lambda_{s2}} A_r(\lambda) d\lambda \Big] . \quad (9)$$

The three coordinates M_R, M_G and M_B of the spectral locus of the perceived colour within an equilateral colour triangle (Fig. 1E) are:

$$\begin{aligned} M_R &= q_R/(q_R + q_G + q_B) , \\ M_G &= q_G/(q_R + q_G + q_B) , \\ M_B &= q_B/(q_R + q_G + q_B) , \end{aligned} \quad (10)$$

for amplitude normalization, and

$$\begin{aligned} M_R &= m_R/(m_R + m_G + m_B) , \\ M_G &= m_G/(m_R + m_G + m_B) , \\ M_B &= m_B/(m_R + m_G + m_B) \end{aligned} \quad (11)$$

for integral normalization. Note that the constants k″ and I_{white} are eliminated from the expressions for M_R, M_G and M_B, as mentioned above. We performed our calculations for both amplitude and integral normalizations, but both conventions provided very similar results. The only significant difference

Fig. 2. Colour picture (intensity and real colour, number of pixels = 560×736=412160) of red flowers and green leaves of *Campsis radicans* (trumpet vine; Bigniniaceae), as recorded with a video camera viewing upward with an elevation of 45° at sunset in the open, when the plant was in the shadow of a house and illuminated from above by light from a clear sky, half of which was visible from the site of the plant. Points 1–12, marked with white or black diamonds, have the following typical spectral and polarizational characteristics used for the calculations in Fig. 5 (Table 1): 1 and 2 = bright green, unpolarized light transmitted through a leaf; 3 and 4 = dark green, weakly polarized light reflected from a leaf; 5 and 6 = bright whitish, blue-green, highly polarized light reflected from a leaf; 7 and 8 = bright red, unpolarized light reflected from a petal; 9 and 10 = bright whitish, red, weakly polarized light reflected from a petal; 11 and 12 = bright whitish, red, medium polarized light reflected from a petal. The graphs in Fig. 3D–F represent data measured along the horizontal white line in this picture. The data measured at the pixel marked here with a white vertical bar are used for the calculations in Figs 7, 8 (Table 2).

between them is that for integral normalization the colour loci remain close to the white point (centre of the colour triangle), i.e. the colours are extremely pale, while for amplitude normalization all colour loci slightly shift towards the red–green border of the colour triangle. The reason for the latter shift is that the integral of $A_G(\lambda)$ is the greatest among the integrals of the absorption curves of the red, green and blue receptors (see Fig. 1A). Hence, when amplitude normalization is used, the quantum absorption q_G of the green receptors is the largest, resulting in the component M_G being the greatest. If integral normalization is used, the relative differences in the quantum absorptions q_R, q_G and q_B of the R-, G- and B-receptors, respectively, are reduced, which decreases the colour saturation. In this study, we present only the results obtained using the more common integral normalization, which puts white in the intuitively correct location in the middle of the colour triangle. The values of the light intensity I_s, the degree of polarization δ_s and the angle of polarization χ_s originate from the reflection-polarization patterns measured by imaging polarimetry in the s = red, green, blue ranges of the spectrum.

Using Equations 10, 11, we computed the coordinates M_r (r=R,G,B) of the colour locus for every pixel of a given picture of plant surfaces. The calculated spectral coordinates M_r were plotted within the equilateral colour triangle (Fig. 1E). Note that the peak wavelengths of the colour receptors in the human eye differ significantly from those of the *Papilio* retina. Thus, the false-colour pictures given in Fig. 4 merely serve to visualize the effect of polarization-induced colour changes for the reader. The false colours will look different to a butterfly.

Results

Fig. 2 shows the colour picture of red flowers and green leaves of a trumpet vine (*Campsis radicans*; Bigniniaceae) at sunset in the open, when the plant was in the shadow and

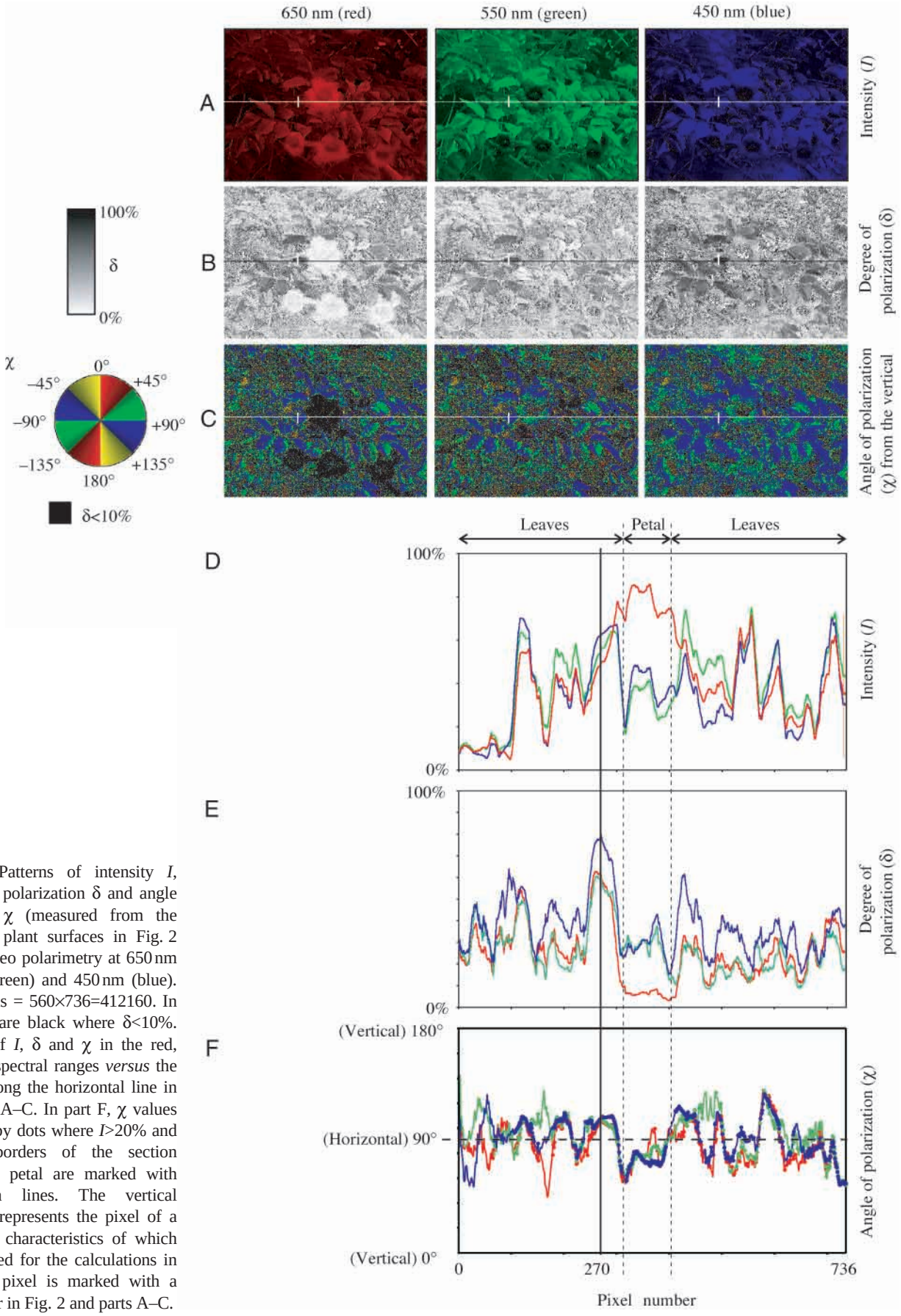

Fig. 3. (A–C) Patterns of intensity *I*, degree of linear polarization δ and angle of polarization χ (measured from the vertical) of the plant surfaces in Fig. 2 measured by video polarimetry at 650 nm (red), 550 nm (green) and 450 nm (blue). Number of pixels = 560×736=412160. In part C, regions are black where δ<10%. (D–F) Graphs of *I*, δ and χ in the red, green and blue spectral ranges *versus* the pixel number along the horizontal line in Fig. 2 and parts A–C. In part F, χ values are represented by dots where *I*>20% and δ>10%. The borders of the section through the red petal are marked with vertical broken lines. The vertical continuous line represents the pixel of a leaf, the optical characteristics of which (Table 2) are used for the calculations in Figs 7, 8. This pixel is marked with a vertical white bar in Fig. 2 and parts A–C.

illuminated from above by light from a clear sky. Fig. 3A–C shows the patterns of intensity I, the degree of linear polarization δ and the angle of polarization χ of this plant measured at wavelengths of 650 nm (red), 550 nm (green) and 450 nm (blue). These patterns contain all the optical information available to a red-, green-, blue- and polarization-sensitive visual system, and they are the inputs for our model retina. In Fig. 3D–F, graphs of I, δ and χ have been plotted against the pixel number from along the horizontal lines shown in Figs 2, 3A–C. The accuracy of the determination of χ is reduced for I<20% and δ<10%; thus, only the χ values represented by dots can be considered as reliable in Fig. 3F.

Fig. 3 shows that the reflectance of the red flower petals of *C. radicans* decreases from the red spectral range towards shorter wavelengths, while the reflectance of the leaves is the highest in the blue and green ranges. The degree of polarization δ of light reflected from the reddish petals is highest in the blue and green ranges ($\delta \approx 30$–40%) and smallest in the red range (δ<10%). Depending on their orientation, leaves reflect partially polarized light with $10\% \leq \delta \leq 80\%$, and δ is the highest in the blue range. In contrast to other leaves, the bright green leaves in the immediate vicinity of the flower at the centre of Fig. 2 (e.g. points 1 and 2) possess very low δ, because the light is not reflected but transmitted through their blades towards the camera, viewing upward with an elevation of 45°; the degree of polarization of transmitted light is reduced owing to diffuse scattering in the leaf tissue. Although the average χ of light reflected from the leaves is about 90° - meaning horizontal polarization, which is the consequence of (i) the illumination (skylight) coming from above and (ii) the approximately horizontal alignment of the majority of the leaf blades - χ often differs considerably from 90° owing to the random and oblique orientation of many leaf blades.

In Fig. 4A, the colours of *C. radicans* are shown as perceived by a polarization-blind retina. They are considered as 'real' colours and serve as a reference; the shifts of the polarization-induced false-colour loci in the colour triangle are measured from the loci of these real colours. Fig. 4B–E shows the false colours of the plant perceived by the weakly polarization-sensitive retina of *P. xuthus* as a function of the alignment α of the dorso-ventral symmetry plane of the eye with respect to the vertical, when a given set of photoreceptors rotates in front of the plant. By rotating the polarization-sensitive receptor set by 180°, the perceived false colours shift continuously in the colour triangle, passing within an approximately elliptical chromatic area; in parts B, C, D and E of Fig. 4 the false colour of the leaves, for example, is slightly blue-green, blue, red and green, respectively. Note that the rectangular images in Fig. 4 are isoluminant, containing information on colour alone (expressing the colour coordinates M_R, M_G and M_B); they give no information on intensity. These colours are, however, more or less masked by the whitish reflected light (see Fig. 2). Similar shifts of the perceived colour occur if the relative position of the plant surface with respect to the receptor set (orientation of the dorso-ventral meridian of the eye) changes because of rotation and/or translation. In the case of *P. xuthus*, the chromatic distances of the polarization-induced false colours from the real colour are small owing to the relatively small polarization sensitivity value (PS=2) of the retina. These chromatic distances are even smaller for the matt petals, which possess a lower δ, than for the shiny leaves, which reflect light with a much higher δ.

Fig. 4 also demonstrates how the real and polarization-induced false colours depend on the orientation of leaf blades. Although the average alignment of leaf blades is approximately horizontal, there are considerable deviations from this direction (see Fig. 3F; the e-vector alignment of specularly reflected light is always perpendicular to the plane of reflection determined by the incident ray, the reflected ray and the normal vector of the reflecting surface). The more or less randomly curved leaf blades are more or less randomly oriented around the horizontal direction, thus both δ and χ change from site to site. The consequence is that the almost homogeneous green real colour of the leaves being independent of δ and χ (see the narrow colour distribution around the most frequent real green colour of leaves in the right colour triangle of Fig. 4A) becomes more heterogeneous for a polarization-sensitive retina, resulting in different colour hues that range from violet (although partly white-masked) through blue, green, yellow and orange to red (see the relatively broad false-colour distribution around the most frequent green false colour of leaves in the colour triangles of Fig. 4B–E). This shows one of the consequences of the polarization sensitivity of colour vision; owing to the high diversity of the degree and angle of polarization of light reflected from plant surfaces, the perceived polarizational false colours are more diverse than the real colours, which is also demonstrated by further examples in Figs 6–8, 10. This phenomenon makes it more difficult to recognize a given real colour and demonstrates a disadvantage of the perception of polarization-induced false colours.

In Fig. 2, six point-pairs of leaves and petals of *C. radicans* that represent typical spectral and polarizational characteristics are selected : In points 1/2, the bright green light transmitted through a leaf is practically unpolarized; in points 3/4, the dark green light reflected from a leaf is weakly polarized; in points 5/6, the bright whitish blue-green light reflected from a leaf is highly polarized; in points 7/8, the bright red light reflected from a petal is practically unpolarized; in points 9/10, the whitish red light reflected from a petal is weakly polarized; and in points 11/12, the bright whitish red light reflected from a petal is moderately polarized. The I, δ and χ values measured at these points are given in Table 1.

Fig. 5 shows the loci of the real colours (beginning of arrows) perceived by a polarization-blind retina and the false colours (arrowheads) perceived by a weakly polarization-sensitive retina for these twelve points within the colour triangle. If the light reflected from or transmitted through a leaf or petal is unpolarized or weakly polarized and has medium or high colour saturation (points 1–4 and 7–10 in Fig. 5), the shift of false colours from the real colours is generally very small. If the light reflected from a leaf or petal is highly polarized and whitish with low colour saturation (points 5, 6, 11 and 12 in

Fig. 5), the differences between the polarization-induced false colours and the real colours are larger than in the former case but remain small.

In *P. xuthus*, the microvilli in the red and green receptors can have three or four different directions, as given in Fig. 1B, and at present it is not known how the receptors contribute to the net neural polarizational signal. It is only known that in the blue receptors, the microvillar direction (β_B) is 0°. Apart from the contribution of β_R=145°, β_G=35° and β_B=0° (Figs 4, 5), we also used other possible combinations of β_R and β_G (together with β_B=0°). Fig. 6D shows how the polarization-induced false colours of an *Epipremnum aureum* plant (golden pothos; Aracea) perceived by *P. xuthus* depend on β_R and β_G. The foreground of Fig. 6A shows the inflorescence of *E. aureum*, which possesses a large, shiny, petal-imitating red leaf called a 'spathe', while the background is composed of the shiny green leaves of the plant. Fig. 6B,C shows the patterns of δ and χ of the plant measured at a wavelength of 450 nm (blue).

Fig. 6 demonstrates the chromatic diversity of the polarizational false colours *versus* the microvillar direction. Depending on β_G and β_R, all false colours (*b–m*) perceived by *P. xuthus* shift slightly towards the red and/or green hues with respect to the real colour *a*, which possesses the largest blue component, M_B. This is because (i) the light reflected from the investigated areas of the plant was approximately horizontally polarized (Fig. 6C) and (ii) the microvillar direction of the blue receptor is dorso-ventrally (vertically) fixed. The false colours are scattered within areas (Fig. 6D), the dimensions of which are similar for both the spathe and

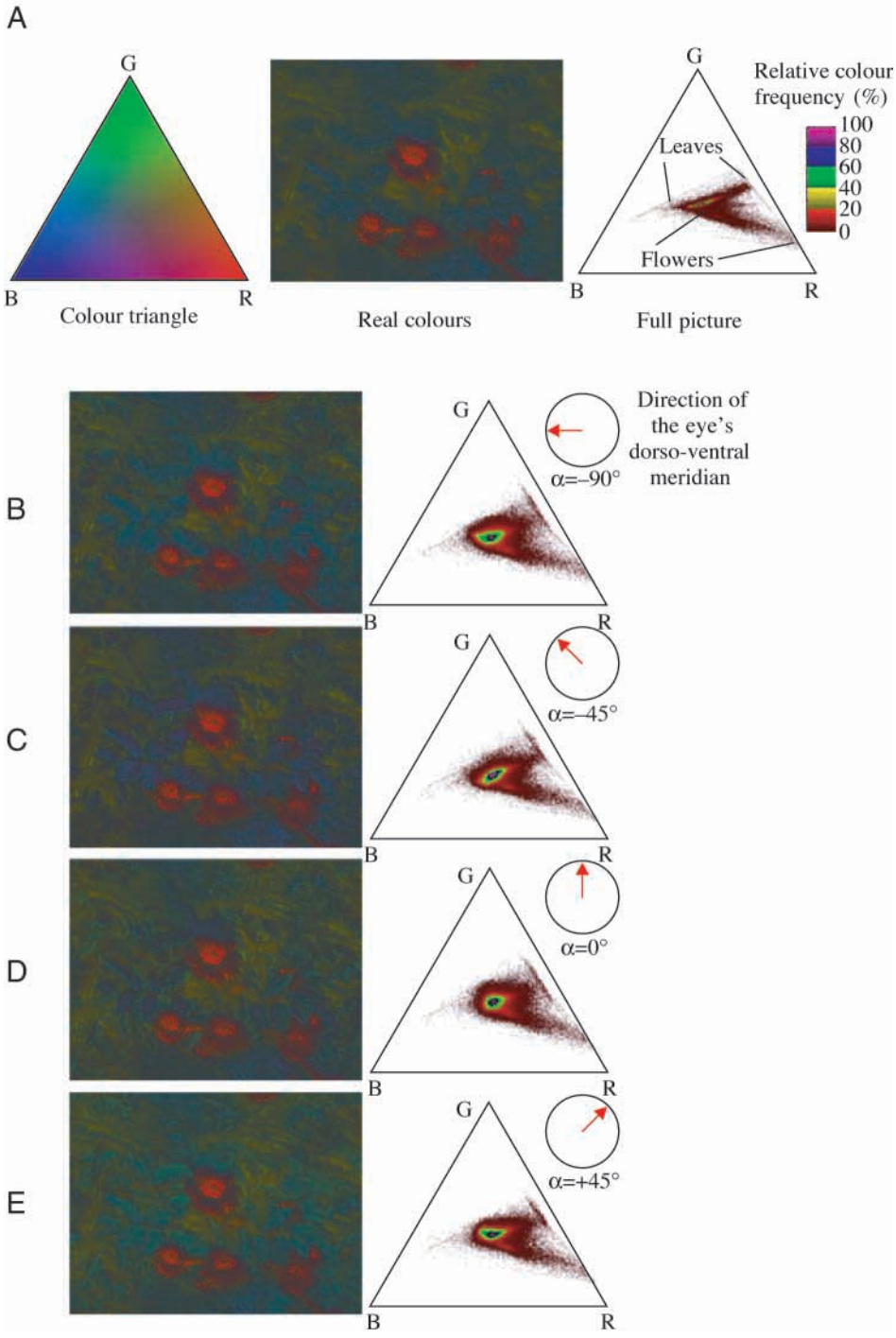

Fig. 4. **(**A**)** Left, equilateral red–green–blue colour triangle filled with the isoluminant colour shades used; middle, real colours of *Campsis radicans* in Figs 2, 3A–C, as perceived by a polarization-blind retina with polarization sensitivity $P_R=P_G=P_B=1$ and microvillar directions β_R, β_G, β_B = arbitrary (number of pixels = 560×736=412160); right, relative frequency distribution of perceived colours (M_R, M_G and M_B) within the colour triangle calculated for the full rectangular picture. Note that the colours used in the white triangles at the right-hand side code the relative frequencies alone and have nothing to do with the perceived colours shown in the rectangular patterns painted by the colours of the colour triangle at the left-hand side in part A. (B–E) Polarization-induced false colours of *C. radicans* perceived by a polarization-sensitive retina with $P_R=P_G=P_B=2$, β_R=145°, β_G=35° and β_B=0°, and their relative frequency distribution in the colour triangle as a function of the alignment α of the eye's dorso-ventral symmetry plane (indicated by red arrows in the circular insets) measured from the vertical. Note that the isoluminant rectangular images and the isoluminant colour triangle on the left in part A give information on colour alone; intensity information is missing.

the leaf because both are shiny and reflect strongly polarized light (Fig. 6B). By changing β_G from 0° to 145°, the false colours *b*, *c*, *d* and *e* (β_R=0°), *f*, *g*, *h* and *i* (β_R=35°) and *j*, *k*, *l* and *m* (β_R=145°), belonging to given values of β_R, are positioned in the colour triangle approximately along straight and parallel lines. By changing β_R from 0° to 145°, the same is true for the false colours *b*, *f* and *j* (β_G=0°), *c*, *g* and *k* (β_G=35°), *d*, *h* and *l* (β_G=90°) and *e*, *i* and *m* (β_G=145°),

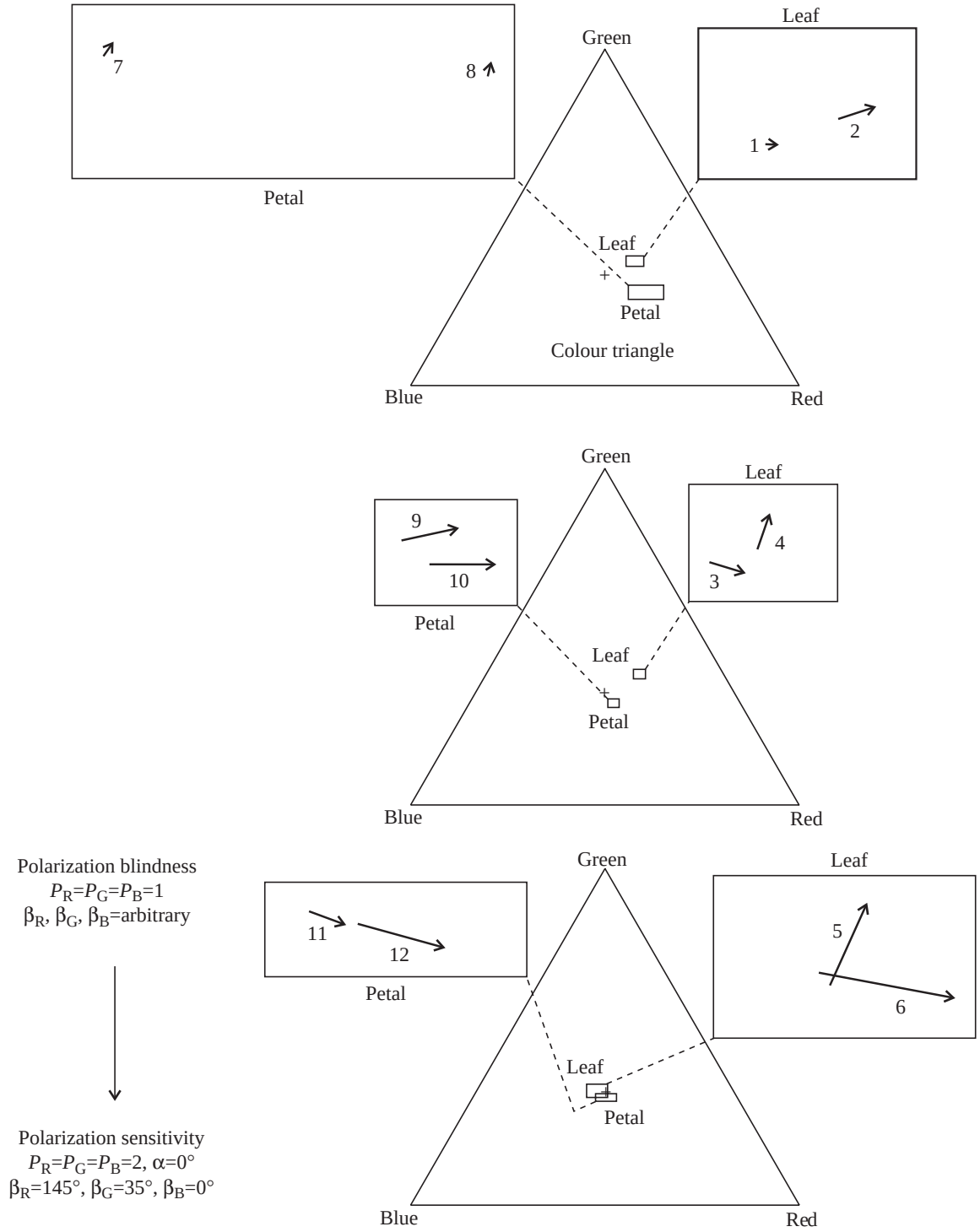

Fig. 5. Spectral loci (M_R, M_G and M_B) of points 1–12 in Fig. 2 plotted within the equilateral red–green–blue colour triangle, the colourless centre of which is represented by +. The rectangular areas of the colour triangle are enlarged and shown next to the triangle, with arrows starting from the spectral locus of real colours perceived by a polarization-blind retina with P_B=P_G=P_R=1 and β_R, β_G, β_B = arbitrary, while the arrowheads point to the spectral locus of false colours perceived by a polarization-sensitive retina with P_B=P_G=P_R=2, α=0°, β_R=145°, β_G=35° and β_B=0°.

Table 1. *Relative intensity* I, *degree of linear polarization* δ *and angle of polarization* χ *(relative to the vertical) of points 1–12 in Fig. 2 measured by video polarimetry at 650 nm (red; R), 550 nm (green; G) and 450 nm (blue; B)*

	I (%)			δ (%)			χ (°)		
Points	R	G	B	R	G	B	R	G	B
1	64	81	41	6	5	18	79	94	118
2	59	75	33	6	5	17	95	168	94
3	29	41	18	9	6	16	91	137	88
4	27	38	15	10	7	19	85	45	102
5	51	62	67	52	45	61	98	96	108
6	61	70	76	33	28	33	80	80	87
7	81	26	21	5	19	30	58	79	61
8	71	27	33	5	21	21	75	73	86
9	65	40	49	8	17	24	94	93	100
10	62	35	44	7	17	24	127	102	96
11	72	67	77	10	12	18	110	107	113
12	59	49	55	15	21	25	108	115	100

These data are used for the calculations in Fig. 5.

Table 2. *Relative intensity* I, *degree of linear polarization* δ *and angle of polarization* χ *(relative to the vertical) of the pixel of a leaf marked with a white vertical bar in Figs 2, 3A–C measured by video polarimetry at 650 nm (red; R), 550 nm (green; G) and 450 nm (blue; B)*

	R	G	B
I (%)	78[a]	87[a]	100[a]
χ (°)	105[a]	107[a]	108[a]
δ_o(R, G, B) (%)	61[a]	59[a]	78[a]
δ_i(R, G, B)=n_i δ_0(R, G, B) (%)			
n_1=0	0[b]	0[b]	0[b]
n_2=0.18	11[b]	10[b]	14[b]
n_3=0.36	22[b]	21[b]	28[b]
n_4=0.55	33[b]	32[b]	42[b]
n_5=0.73	44[b]	43[b]	57[b]
n_6=0.91	55[b]	53[b]	71[b]
n_7=1.09	66[b]	64[b]	85[b]
n_8=1.28	78[b]	75[b]	99[b]

[a]These data are used for the calculations in Fig. 7.

[b]Using the original degrees of polarization δ_0, the enhanced degrees of polarization are derived as follows: $\delta_i=n_i\delta_0$, i=1–8, where n_i is an arbitrary factor. These data are used for the calculations in Fig. 8.

belonging to given values of β_G. The angle between these lines is about 120°.

Having based our previous considerations on a low polarization sensitivity of *PS*=2, let us now consider visual systems with high *PS* values. High *PS* values have been measured in the specialized dorsal rim area of the compound eye of several insects: *PS*≈10 in honeybees *A. mellifera* (Labhart, 1980) and in crickets *G. campestris* (Blum and Labhart, 2000). Apart from the dorsal rim area, high *PS* values (mean *PS*=7) were found in the lateral retina of waterstriders (*Gerris lacustris*; Bartsch, 1995). Fig. 7 shows the dependence of the polarization-induced false colours on $P_B=P_G=P_R=P$ as a function of β_G and β_R. When *P* increases from 1 to 20, all false colours shift to some degree from the real unsaturated, bluish-green colour (locus *a*) of the leaf towards relatively saturated red, orange, yellow or green colours. The chromatic distance of the false colours from the real colour can be considerable if the polarization sensitivity is strong enough.

The degree of polarization δ of light reflected from plant surfaces depends on the angle of incidence, the surface roughness and the wavelength. At wavelengths where the amount of light coming from the subsurface layers is negligible in comparison with the amount of light reflected from the surface, the reflected light can be almost totally polarized if the angle of incidence is near the Brewster angle (Horváth and Varjú, 1997). This is the situation for shiny green leaves in the blue or red range of the spectrum (Fig. 3), for instance. The increasing surface roughness decreases the δ. Hence, in natural conditions, the δ of light reflected from plant surfaces can vary between 0% and almost 100%. Fig. 8 shows the dependence of the polarization-induced false colour on the δ of reflected light as a function of β_G and β_R.

Comparing Fig. 8 with Fig. 7, we see that the dependence of the polarization-induced false colours on the δ (Fig. 8) is qualitatively the same as that on the polarization sensitivity *P* of the photoreceptors (Fig. 7). The only essential quantitative difference between Fig. 7 and Fig. 8 is that, in the latter, the chromatic shifts (the lengths of the arrows) are much smaller than in the former, in spite of the very high δ values of 78%, 75% and 99%.

Fig. 9 shows how the spectral and polarizational characteristics of a sunlit leaf of a *Ficus benjamina* tree (weeping fig; Ficaceae) depend on the direction of the sunlight at a given solar elevation and how they change if the leaf is shaded from direct sunlight. The colours, as well as the δ and χ of light reflected from the leaf, depend on the orientation of the leaf blade with respect to the sun. For a given position of the sun, there are chromatic and polarizational differences between the sunlit and the shaded leaves. The colour of the sunlit leaf is always greenish (Fig. 9A,C,E,G) owing to the diffuse scattering and selective absorption of white sunlight in the green subcuticular leaf tissue. This greenish hue is, however, more or less masked by strong specular reflection of white sunlight if the leaf is viewed in the direction of the sun (Fig. 9G). The colour of the shaded leaf (Fig. 9B,D,F,H) is always bluish, because it is illuminated by blue skylight. Owing to the non-planar, curved shape of the leaf blade, the δ and χ of reflected light changes from point to point. In Fig. 9, the leaf blade in the small rectangular left and right window is approximately horizontal and vertical, respectively. Note that, although in Fig. 9G the entire leaf is lit by direct sunlight, both the left and right windows are placed in a local shaded region because of the curved leaf blade. Thus, both the left and right windows in Fig. 9G represent a shaded situation.

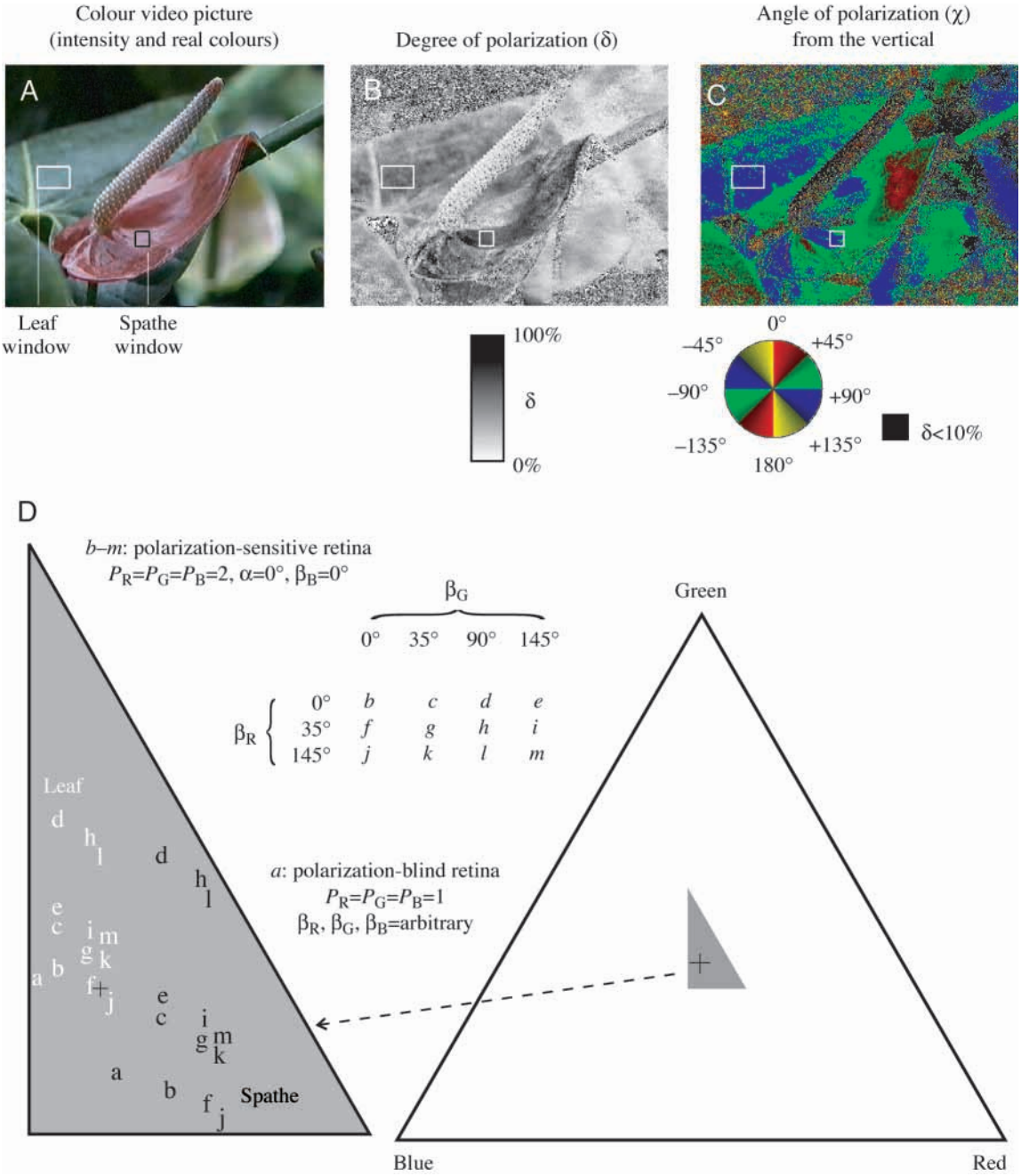

Fig. 6. **(**A–C**)** Colour picture and the patterns of the degree δ and angle χ of polarization of *Epipremnum aureum* (Aracea) - illuminated by light from a full clear sky from above through the glass panes of a greenhouse - measured by video polarimetry at a wavelength of 450 nm (blue). In part C, the regions are represented in black where δ<10%. Number of pixels = 560×736=412160. (D) Colours (M_R, M_G and M_B) of *E. aureum* perceived by a polarization-blind retina, with $P_B=P_G=P_R=1$, and β_R, β_G, β_B = arbitrary (*a*), and by a polarization-sensitive retina, with $P_B=P_G=P_R=2$, α=0°, $\beta_B=0°$ as a function of the microvillar directions β_G and β_R of the green and red receptors (*b–m*). Every microvilli situation is designated by a letter ranging from *a* to *m*. The corresponding spectral loci (designated by letters *a–m*) of two details of the picture, one on a leaf blade (white) and one on the spathe (black) marked by rectangular windows in patterns A–C, are plotted within the equilateral R–G–B colour triangle, the colourless centre of which is represented by +.

In Fig. 10, we can see that, under the clear blue sky, the hues of shaded leaves are always nearer to the blue-green parts of the colour triangle than those of sunlit leaves. In the left window of the leaf in Fig. 9, the false colour shifts (represented by arrows) towards red, orange, yellow or green hues for both shaded and sunlit leaves. In the right window of the leaf in Fig. 9, because the orientation of the leaf blade is different (vertical) from that in the left window (horizontal), the colour shifts in the right window differ from those in the left window. Apart from Fig. 9E in the right window, the false colours shift

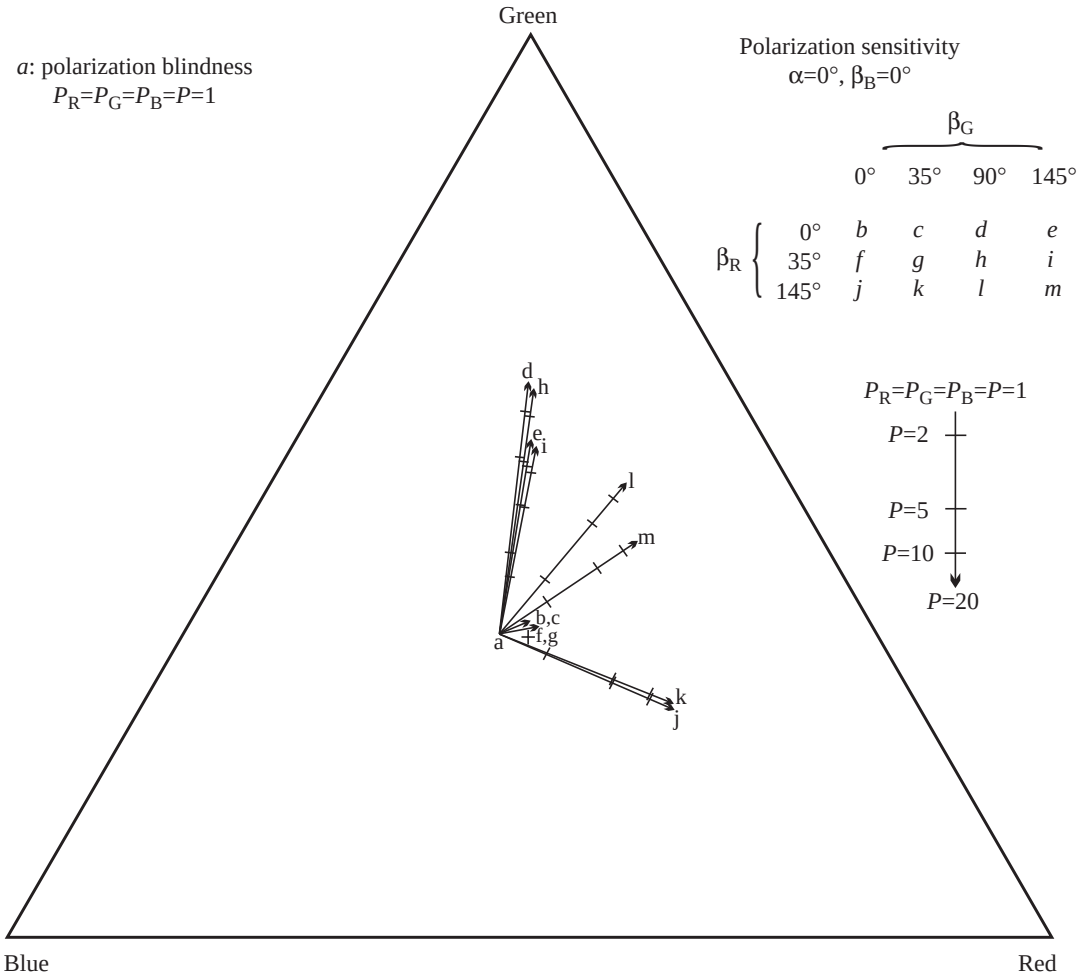

Fig. 7. Dependence of the polarization-induced false colour (M_R, M_G and M_B) perceived by a retina with $\alpha=0°$, $\beta_B=0°$ on the polarization sensitivity $P_B=P_G=P_R=P$ as a function of the microvillar directions β_G and β_R of the green and red receptors (designated by letters *b*–*m*) plotted within the equilateral R–G–B colour triangle, the colourless centre of which is represented by +. The colours are calculated for a point on a leaf of *Campsis radicans* marked by a white vertical bar in Figs 2, 3A–C. The reflection-polarization characteristics of this point are given in Table 2. The arrows start from the spectral locus *a* of the real colour when $P_B=P_G=P_R=1$, meaning polarization-blindness, while the arrowheads point to the spectral locus of perceived false colours if $P_B=P_G=P_R=P=20$. The spectral loci of false colours for *P* values ranging from 1 to 20 are placed along the straight arrows, on which the loci for $P=2$, $P=5$ and $P=10$ are marked by bars.

towards the green hues for both shaded and sunlit leaves. In Fig. 9E, the colour shift is very small.

Discussion

Reflection-polarization characteristics of plant surfaces

In the present study, we investigated the false colours induced by the partially linearly polarized light reflected from plant surfaces in a polarization-sensitive trichromatic colour vision system. We thus continued the analysis done by Wehner and Bernard (1993) and applied it in particular to the weakly polarization-sensitive retina of *Papilio* butterflies. Moreover, we performed an imaging polarimetric approach. As expected, the higher the degree of polarization δ, the stronger the colour shift, the direction of which depends on the viewing direction, the alignment of the dorso-ventral meridian of the eye, the polarization sensitivity, the microvillar orientation of the photoreceptors and the illumination conditions.

Rough surfaces reflect light diffusely, which reduces polarization. Thus, the rougher a plant surface (e.g. owing to a waxy layer or other microstructures), the lower the δ of reflected light. The e-vector reflected from a plant surface follows its curvature, because the reflected light becomes partially linearly polarized perpendicularly to the plane of reflection for any dielectric (non-metallic) reflector.

The darker a plant surface in a given spectral range, the higher the δ of reflected light. The reason for this is as follows. The δ of light reflected by the cuticle or epidermis of plants depends on the incident angle but is almost independent of the wavelength. The e-vector of reflected light is parallel to the surface. The colour of plant surfaces arises from the selective absorption and diffuse scattering of light in the tissue below

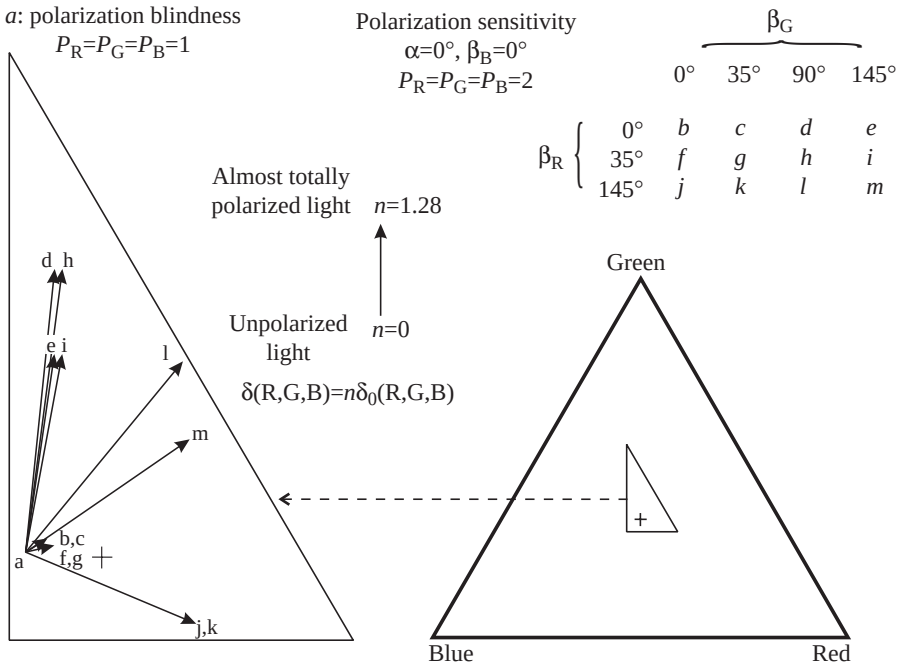

Fig. 8. Dependence of the polarization-induced false colour (M_R, M_G and M_B) perceived by a polarization-sensitive retina with $P_B=P_G=P_R=2$, $\alpha=0°$, $\beta_B=0°$ on the degree of polarization δ(R,G,B) of reflected light as a function of the microvillar directions β_G and β_R of the green and red receptors (designated by letters *b*–*m*) plotted within the equilateral R–G–B colour triangle, the colourless centre of which is represented by +. The colours are calculated for the point of a leaf of *Campsis radicans* marked by a white vertical bar in Figs 2, 3A–C. The original reflection-polarization characteristics of this point are given in Table 2. The degrees of polarization of reflected light are calculated as $\delta(R,G,B)=n\delta_0(R,G,B)$ and given in Table 2, where *n* is an arbitrary factor. The arrows start from the spectral locus *a* of the real colour when $n=0$ (unpolarized light) and $P_B=P_G=P_R=P=1$ (polarization blindness), while the arrowheads point to the spectral locus of perceived false colours for $n=1.28$ (almost totally polarized light in all three spectral ranges). The spectral loci of false colours for *n* values ranging between 0 and 1.28 are placed approximately equidistant along the straight arrows.

the transparent cuticle. The diffuse light emanating from this tissue is originally unpolarized, but it becomes partially polarized after transmission and refraction at the epidermis. The e-vector of the tissue-scattered light is perpendicular to the cuticle because of refraction polarization (Horváth and Varjú, 1997). Hence, the net degree and direction of polarization of a plant surface are determined by the superposition of the epidermis-reflected and the subcuticle-scattered light. If the former dominates (e.g. in sunlit shiny leaves observed from the direction of specular reflection), the direction of polarization is parallel to the cuticle; otherwise, the e-vector is perpendicular to it (e.g. sunlit leaves observed from behind, when the leaf-transmitted light is perceived). In those spectral regions where the subcuticle-scattered light has a considerable contribution to net polarization, the net δ of the returned light is reduced or even abolished.

These general rules are demonstrated in Fig. 3. The considerably reduced amount of subcuticle-scattered light in the blue range causes the red flowers to be dark and relatively strongly polarized at 450 nm and 550 nm (Fig. 3E). At 650 nm, the amount of light emanating from the red tissue below the epidermis of the flower is greater; thus, the net δ is reduced. This is the physical reason for the general rule that, in a given spectral region, the darker objects polarize light to a higher degree if the illuminating light is unpolarized and white. Thus, green leaves are less polarized in the green range than in the blue and the red ranges, as can be well seen in Fig. 3.

In Fig. 2, we selected three point-pairs of both leaves and petals for calculating polarization-induced false colours. At point-pairs 5/6 and 11/12 (Table 1), δ is relatively high owing to the large amount of skylight reflected from the cuticle as well as to an alignment of the plant surface resulting in an angle of view near the Brewster angle. However, the colour saturation is low owing to the interference with the cuticle-reflected whitish/bluish skylight and the tissue-backscattered greenish or reddish light. At point pairs 1/2, 3/4, 7/8 and 9/10 in Fig. 2 (Table 1), the situation is reversed: δ (in the dominant wavelength range) is low owing to the small amount of skylight reflected from the cuticle as well as to an alignment of the plant surface resulting in an angle of view far from the Brewster angle, but the colour saturation is higher because the amount of cuticle-reflected skylight is small.

Surfaces of petals have a matt finish, making them much better diffuse reflectors than leaves, which have a shiny, smooth cuticle (Kay et al., 1981; Wehner and Bernard, 1993). Thus, petals usually reflect diffuse and only weakly polarized light, while leaves reflect more specularly (i.e. the angle of incidence is the same as the angle of reflection, and the reflected light is in the plane determined by the incident light and the normal vector of the surface) and the reflected light is generally highly polarized if the direction of view is near the Brewster angle.

We propose that the major function of the surface roughness of petals is not to reduce the δ of reflected light (and thus to reduce the polarization-induced false colours) but to reduce the white glare of the surface, which would overwhelm the petal-tissue-backscattered coloured light and would make it more difficult to perceive the real, attractive and striking colour of the petal. An appropriately rough petal surface functions as a Lambertian reflector, which reflects light uniformly in all directions independent of the angle of incidence. As a by-product, the light reflected by a Lambertian surface is

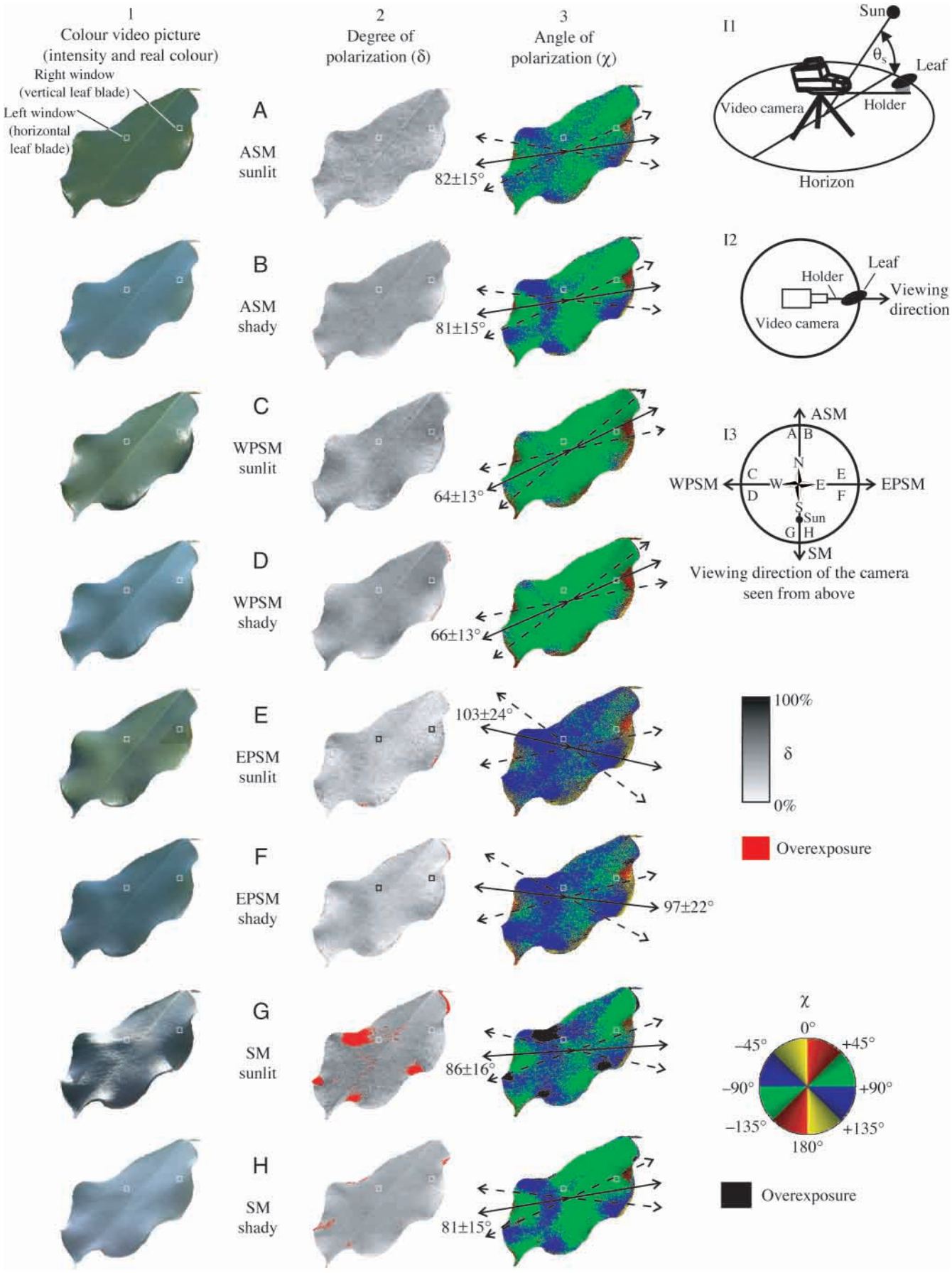
1
Colour video picture
(intensity and real colour)
Right window
(vertical leaf blade)
Left window
(horizontal
leaf blade)
2
Degree of
polarization (δ)
3
Angle of
polarization (χ)
A
ASM
sunlit
82±15°
B
ASM
shady
81±15°
C
WPSM
sunlit
64±13°
D
WPSM
shady
66±13°
E
EPSM
sunlit
103±24°
F
EPSM
shady
97±22°
G
SM
sunlit
86±16°
H
SM
shady
81±15°
I1
Sun
θs
Leaf
Video camera
Holder
Horizon
I2
Holder
Leaf
Viewing
direction
Video camera
I3
ASM
WPSM
EPSM
SM
Sun
Viewing direction of the camera
seen from above
100%
δ
0%
Overexposure
χ
0°
+45°
+90°
+135°
180°
–135°
–90°
–45°
Overexposure

Fig. 9. Spectral and reflection-polarization characteristics of a leaf of a *Ficus benjamina* tree (Ficaceae) as functions of the illumination conditions in the open. The leaf was mounted in front of the camera on a horizontal rod (holder), which rotated in a horizontal plane around a vertical axis together with the camera (insets I1 and I2). The solar elevation was θ_S=55°, and the leaf was illuminated by direct sunlight (parts A, C, E and G) or shaded with a small screen that just occluded the sun and exposed the leaf to the full clear sky (parts B, D, F and H) . In the small rectangular left and right window, the leaf blade is approximately horizontal and vertical, respectively. Inset I3 shows the four different horizontal directions of view of the camera with respect to the solar azimuth. ASM, antisolar meridian; SM, solar meridian; EPSM, eastwardly perpendicular to the solar meridian; WPSM, westwardly perpendicular to the solar meridian. Column 1 shows colour video pictures of the leaf. Column 2 shows patterns of the degree of linear polarization δ of the leaf measured by video polarimetry at a wavelength of 450 nm (blue). Column 3 shows patterns of the angle of polarization χ (measured from the vertical) of the leaf at a wavelength of 450 nm, where the dominant (average) electric field vector alignment of the leaf blade is represented by a solid arrow, and the standard deviations are represented by broken arrows.

unpolarized. The intensity and colour of such a (matt) Lambertian surface is the same from all directions of view. If the surface of a petal were smooth, like the red spathe in Fig. 6A, it would function as a Fresnel reflector, which reflects light specularly. Then, the intensity and colour of the petal-tissue-backscattered coloured light would be overwhelmed by the white glare (i.e. by the specularly reflected white light) from the smooth cuticle if the direction of view coincides with the angle of reflection. This problem would not occur for other directions of view. Hence, the reduction of the δ of reflected light seems to be the consequence, and not the main aim, of the surface roughness of petals. The roughness of petal surfaces is of great importance for all colour vision systems, independent of polarization blindness or polarization sensitivity, which must efficiently detect and distinguish the colours of flowers.

In columns 2 and 3 of Fig. 9, we can see that, at a given illumination direction and in a given (e.g. blue) part of the spectrum, the gross features of the patterns of δ and χ of the *F. benjamina* leaf are similar for both sunlit and shaded cases, although the colours of the sunlit and shaded leaf differ considerably. This is because the smooth *F. benjamina* leaf is similar to a Fresnel reflector, and the leaf blade is tilted so that sunlight cannot be reflected specularly from it towards the camera (apart from certain small curved areas). Thus, the sunlight reflected specularly from the leaf blade is not visible and does not add to the leaf-tissue-backscattered light. Large differences between the reflection-polarization characteristics of sunlit and shaded leaves occur only if the direction of view coincides with or is near to the direction of specular reflection. This is seen at those regions of the *F. benjamina* leaf shown in Fig. 9G,H, where, owing to the appropriate local orientation of the curved leaf blade, the sunlight is specularly reflected. The consequence of this is that, in a considerable portion of these areas, the leaf blade is overexposed owing to the too-bright reflected sunlight.

All our findings are in accord with the earlier results of Shul'gin and Moldau (1964), Vanderbilt and Grant (1985a, b), Vanderbilt et al. (1985a, b), Grant (1987), Grant et al. (1987a, b, 1993) and Sarto et al. (1989), who measured the polarized, non-polarized and specular reflectance of leaves of many different plant species as functions of the leaf surface features in the visible and near-infrared parts of the spectrum by point-source polarimetry. They found that in some viewing directions the surface reflection is so large that leaves appear white instead of green. In this case, the strong specularly surface-reflected white light overwhelms the much smaller

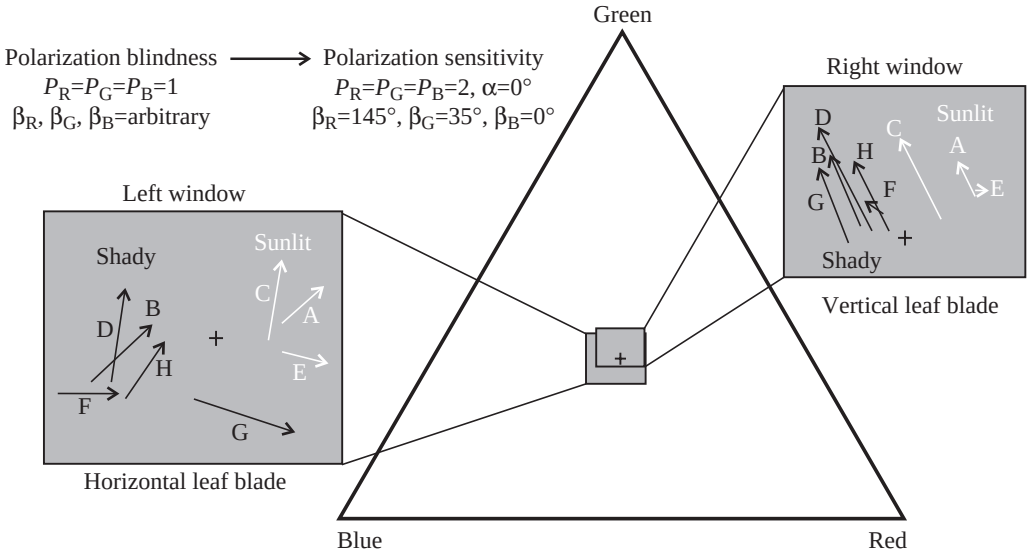

Fig. 10. Spectral loci (designated by A–H, representing the situations A–H in Fig. 9) of the leaf areas marked with a left and a right small rectangular window in Fig. 9 plotted within the equilateral R–G–B colour triangle, the colourless centre of which is represented by +. The arrows start from the spectral locus of real colours perceived by a polarization-blind retina with $P_B=P_G=P_R=1$ and β_R, β_G and β_B = arbitrary, while the arrowheads point to the spectral locus of false colours perceived by a polarization-sensitive retina with $P_B=P_G=P_R=2$, α=0°, β_R=145°, β_G=35° and β_B=0°.

amount of green light scattered diffusely by the interior leaf tissue. They showed that the reflectance of the colourless and transparent leaf epidermis is practically independent of the wavelength of light, and, in the visible part of the spectrum, the degree of polarization of light reflected from green leaves is always the lowest in the green spectral range. They also demonstrated that the whitish light reflected specularly from leaves is always strongly polarized, while the green light reflected diffusely and non-specularly is practically unpolarized.

Do polarization-induced false colours influence the colour vision of Papilio *butterflies under natural conditions?*

Figs 4–8, 10 clearly show that, for our weakly polarization-sensitive model retina, the polarization-induced false colours of plants fall near the real colours perceived by a polarization-blind retina, even if they reflect strongly polarized light. Another effect of specular reflection is that whitish glare strongly masks the colour hue. Is the colour vision system of *Papilio* butterflies sensitive enough to perceive the tiny polarization-induced colour shifts in Figs 4–8, 10 under these circumstances? Behavioural studies on the discrimination of weakly saturated colours by insects are scarce. Honeybees seem to be able to discriminate pure white from white mixed with just a few percent of spectral light (Daumer, 1963; Lieke, 1984). Such stimuli differ in their locus position to a comparable degree, as the loci of the real colours differ from some of the polarizational false colours calculated in this study. However, how well *Papilio* discriminates unsaturated colours remains to be demonstrated.

In plant parts with dominating diffuse reflection, the colour saturation is relatively high but the δ is low (Table 1). Although in this case hue discrimination will be good, the false colour effect is minute (1–4 and 7–10 in Fig. 5). Thus, under natural conditions, the weak polarization sensitivity of the photoreceptors might not interfere with the colour vision at all. This may be the reason why the average *PS* value of the photoreceptors in proven colour-sensitive insects is not reduced to 1.0 but is found to be approximately 2.0–2.5 (*Cataglyphis bicolor*, Labhart, 1986; *Papilio*, Kelber et al., 2001; *Drosophila melanogaster*, Speck and Labhart, 2001; other fly species, Hardie, 1985). Only in honeybees is the *PS* value significantly smaller than 2 (Labhart, 1980). The complete destruction of the polarization sensitivity in a microvillar photoreceptor is not a trivial task but calls for a systematic misalignment of the microvilli along the rhabdom, in which complicated optical effects such as self-screening and lateral filtering within the rhabdom must be considered. The microvilli are misaligned by random or continuous direction changes (twisting) along the rhabdom, but, in most photoreceptors, certain microvillar directions still dominate (reviewed by Labhart and Meyer, 1999). In honeybees, the rhabdom twists by about 180°, which reduces the *PS* to lower values than in other insects (Wehner et al., 1975; Labhart, 1980). This might be taken as an indication that the exquisite colour vision system of honeybees might be more sensitive to small colour differences than that of other insect species and, thus, be more compelled to avoid polarizational false colours.

Recently, Kelber (1999a) and Kelber et al. (2001) showed that the colour choices of butterflies *P. aegeus* and *P. xuthus* is influenced by the e-vector orientation of linearly polarized light emitted by the colour stimuli to which the butterflies are exposed. They suggested that the interaction between colour and polarization might help the butterfly to find the best oviposition sites. Thus, horizontally polarized green stimuli (mimicking horizontally oriented green leaves) were more attractive than vertically polarized stimuli of the same colour. At first glance, the findings of Kelber and collaborators – that polarization influences the colour choices of *Papilio* butterflies – seem to contradict our conclusion that colour vision is quite insensitive to reflection polarization. However, in their behavioural tests, the authors used stimuli that had both a very high degree of polarization (almost 100%) and a high degree of colour saturation, a situation that does not occur under natural conditions. Using this hyperstrong polarization/colour saturation combination, Kelber (1999a) and Kelber et al. (2001) confirmed behaviourally the polarization sensitivity of the *Papilio* photoreceptors that was previously measured electrophysiologically (Bandai et al., 1992). We assume that this receptor property plays only a minor role in real life. To demonstrate that the polarization sensitivity of the colour vision system can indeed ease certain vital tasks in the life of a butterfly, further behavioural experiments with *Papilio* exposed to stimuli with natural combinations of degree of polarization and colour saturation are needed. It is currently unknown how large a false colour shift needs to be in order to be just detectable and thus useful in a behavioural context. Although we do not claim that our calculations prove that *Papilio* is incapable of detecting false colours under natural conditions, we expect that the calculated colour shifts in the simulated *Papilio* retina are not large enough to be perceived. The question of whether *Papilio* is equally sensitive to colours as bees and could perceive spectral shifts comparable with the polarizational false colour shifts calculated in this work can be answered only by further studies of the colour sensitivity of *Papilio*.

Another finding that seems to contradict our thesis is that, in plants, the petals are usually less shiny than the leaves (Kay et al., 1981); i.e. specular reflection is reduced relative to diffuse reflection and, therefore, they exhibit less polarization. One might argue that this is to reduce false colour effects and, thus, to improve flower recognition. However, matter petals also avoid masking of the hue of a flower by whitish glare. The avoidance of glare alone may already be reason enough to reduce specular reflection in petals: the matter the petals, the more constant the appearance of flower colour when seen from different directions.

Limitations of our polarimetric technique and retina model and their consequences

Papilionid butterflies have a pentachromatic colour vision system, which was discovered by Arikawa et al. (1987). Thus,

taking into account only three of the five known receptor types seems to be an over-simplification and does not represent the exact (possibly five-dimensional) colour space of the animal. We admit that our approach has inherent limitations: our polarimetric technique cannot measure the reflection-polarization characteristics of plant surfaces in the UV, and our retina model disregards the violet (V) and UV receptor types. However, these do not destroy the utility of our approach and, by no means, the validity of our conclusions owing to the following reasons.

First, the optical phenomenon – that low degrees of polarization of light reflected from plant surfaces are always associated with high colour saturations, and strongly polarized reflected light is necessarily associated with low colour saturation – is valid for both the UV and visible ranges of the spectrum. Although demonstrated in the visible spectrum only, there is no physical reason why this phenomenon should not occur in the UV. Hence, the wavelength limitations of our instrument do not restrict the mentioned phenomenon to the visible spectrum. Second, the two reasons for the small differences between the real and polarizational false colours of plant surfaces calculated in this work are the above-mentioned optical phenomenon and the weak polarization sensitivity of the *Papilio* photoreceptors. Involving also the violet and UV receptors in an improved pentachromatic retina model and using additional reflection-polarization data measured by a UV-sensitive polarimeter would not result in larger shifts of polarization-induced false colours with respect to the corresponding real colours. This would only change the position of the colour loci but not the magnitude of chromatic differences. For instance, our retina model could be improved in such a way that the spectral sensitivity function of the 'short wavelength macro-receptor' compressing the UV, violet and blue (B) receptors with the same microvilli orientation is chosen to be much broader (e.g. stretching from 300 nm to 550 nm) than that of the blue receptor in Fig. 1A. However, the only effect of the enhanced sensitivity of this macro-receptor on the colour calculations would be a shift of all real and polarizational false colours towards the short-wavelength range of the spectrum, while their chromatic distances would not change significantly and would remain small henceforward. Varying the number of receptor types involved in the model retina and changing their spectral sensitivity functions can drastically alter the loci of the real and polarizational false colours as well as their relative directions within a multi (3, 4 or 5)-dimensional colour space but has only a minor influence on the chromatic distances of the false colours from the corresponding real colours. This was quantitatively shown as follows: all colour calculations for our trichromatic model retina using integral normalization of the red, green and blue sensitivity functions (Fig. 1A) were repeated using amplitude normalization (see Materials and methods). Practically the only effect of this normalization switch was that all colours shifted towards the green–red border of the R–G–B colour triangle without significant changes of their chromatic distances or relative directions, although the switch did result in significant changes in the relative spectral sensitivity functions.

In our retina model the UV, violet and blue receptors can be treated as one receptor type owing to the following:

(i) Among the five *Papilio* receptor types, the largest overlapping areas occur between the sensitivity functions of the UV, violet and blue receptors (Kelber et al., 2001), resulting in a high colinearity of the quantum absorptions of these receptors. Furthermore, the UV, violet and blue receptors have the same microvillar orientation, $\beta=0°$ (Kelber et al., 2001). Therefore, compressing these three short-wavelength receptors into a single macro-receptor results in the least simplification considering the sensitivity functions and microvilli orientations in the trichromatic receptor model.

(ii) Kelber (1999b) investigated experimentally the spectral preference of *P. aegeus* for oviposition stimuli and found that at least three receptor types contribute to the behaviour: the green receptor with a positive sign, the red receptor with a negative sign and at least one of the three short-wavelength receptors with a negative sign. She also developed five-, four, three- and two-receptor models to describe the choice behaviour of egg-laying *Papilio* in terms of linear interactions among the different spectral types of photoreceptors. It was found that of the three-receptor retina models, the R–G–B model fitted the experimental data best, although it differed significantly from the five-receptor model. It was concluded that colour choice for oviposition in *Papilio* is guided by a single chromatic mechanism, that the most parsimonious retina model is the R–G–B model, predicting correctly the choice behaviour of the animals, and that the full R–G–B–V–UV model describes the multiple choice data only slightly better. Thus, the simplification caused by involving in our retina model only the R, G and B receptor types may influence only slightly our conclusions about the effect of polarizational false colours on the colour-choice behaviour of *Papilio* butterflies.

(iii) In a study of the polarization dependence of colour vision in *P. aegeus* (colour choice in oviposition behaviour) and *P. xuthus* (colour choice in feeding behaviour), Kelber et al. (2001) displayed the colour loci of the stimuli in colour triangles, which represent the B, G and R receptors and are a projection of the maximum five-dimensional colour space of *Papilio* spp. onto the two-dimensional plane of the sheet of paper, disregarding the UV and violet receptors and the light intensity. This allowed them to visualize the influence of polarization on perceived colour under different assumptions. Following their approach in the present work seems, thus, legitimate.

This work was supported by a Humboldt research fellowship from the German Alexander von Humboldt Foundation and by an István Széchenyi fellowship from the Hungarian Ministry of Education to G. Horváth, as well as by a doctoral fellowship received by J. Gál from the George Soros Foundation (grant number 230/2/878). The grant 31-43317.95 from the Swiss National Science Foundation to R. Wehner is gratefully acknowledged. Many thanks are to Dr

Almut Kelber for reading and commenting on earlier versions of the manuscript. We are also grateful to two anonymous reviewers for their constructive comments and criticism. A part of this work was written at the Department of Cognitive Neuroscience of the University of Tübingen (Germany), where G. Horváth spent his Humboldt fellowship. Thanks to Prof. Hanspeter Mallot (Head of Department) for his support.

References

Arikawa, K., Inokuma, K. and Eguchi, E. (1987). Pentachromatic visual system in a butterfly. *Naturwissenschaften* **74**, 297-298.

Bandai, K., Arikawa, K. and Eguchi, E. (1992). Localization of spectral receptors in the ommatidium of butterfly compound eye determined by polarisation sensitivity. *J. Comp. Physiol. A* **171**, 289-297.

Bartsch, K. (1995). Polarization-sensitive photoreceptors of different spectral types in the compound eye of waterstriders. *Naturwissenschaften* **82**, 292-293.

Blum, M. and Labhart, T. (2000). Photoreceptor visual fields, ommatidial array, and receptor axon projections in the polarization-sensitive dorsal rim area of the cricket compound eye. *J. Comp. Physiol. A* **186**, 119-128.

Daumer, K. (1963). Kontrastempfindlichkeit der Bienen für Weiss verschiedenen UV-Gehalts. *Z. vergl. Physiol.* **46**, 336-350.

Grant, L. (1987). Diffuse and specular characteristics of leaf reflectance. *Remote Sens. Env.* **22**, 309-322.

Grant, L., Daughtry, C. S. T. and Vanderbilt, V. C. (1987a). Polarized and non-polarized leaf reflectances of *Coleus blumei*. *Env. Exp. Bot.* **27**, 139-145.

Grant, L., Daughtry, C. S. T. and Vanderbilt, V. C. (1987b). Variations in the polarized leaf reflectance of *Sorghum bicolor*. *Remote Sens. Env.* **21**, 333-339.

Grant, L., Daughtry, C. S. T. and Vanderbilt, V. C. (1993). Polarized and specular reflectance variation with leaf surface features. *Phys. Planta.* **88**, 1-9.

Hardie, R. C. (1985). Functional organization of the fly retina. In *Progress in Sensory Physiology*, vol. 5 (ed. H. Autrum et al.), pp. 2-79. Berlin, Heidelberg, New York: Springer.

Horváth, G. and Varjú, D. (1997). Polarization pattern of freshwater habitats recorded by video polarimetry in red, green and blue spectral ranges and its relevance for water detection by aquatic insects. *J. Exp. Biol.* **200**, 1155-1163.

Kay, Q. O. N., Daoud, H. S. and Stirton, C. H. (1981). Pigment distribution, light reflection and cell structure in petals. *Bot. J. Linnean Soc.* **83**, 57-84.

Kelber, A. (1999a). Why 'false' colours are seen by butterflies. *Nature* **402**, 251.

Kelber, A. (1999b). Ovipositing butterflies use a red receptor to see green. *J. Exp. Biol.* **202**, 2619-2630.

Kelber, A., Thunell, C. and Arikawa, K. (2001). Polarisation-dependent colour vision in *Papilio* butterflies. *J. Exp. Biol.* **204**, 2469-2480.

Labhart, T. (1980). Specialized photoreceptors at the dorsal rim of the honey bee's compound eye: polarizational and angular sensitivity. *J. Comp. Physiol.* **141**, 19-30.

Labhart, T. (1986). The electrophysiology of photoreceptors in different eye regions of the desert ant, *Cataglyphis bicolour*. *J. Comp. Physiol. A* **158**, 1-7.

Labhart, T. and Meyer, E. P. (1999). Detectors for polarized skylight in insects: a survey of ommatidial specializations in the dorsal rim area of the compound eye. *Microsc. Res. Tech.* **47**, 368-379.

Lieke, E. (1984). *Farbensehen bei Bienen: Wahrnehmung der Farbsättigung.* Ph.D. Thesis, Freie Universität Berlin, Berlin.

Lunau, K. and Maier, E. J. (1995). Innate colour preferences of flower visitors. *J. Comp. Physiol. A* **177**, 1-19.

Przyrembel, C., Keller, B. and Neumeyer, C. (1995). Trichromatic colour vision in the salamander (*Salamandra salamandra*). *J. Comp. Physiol. A* **176**, 575-586.

Sarto, A. W., Woldemar, C. M. and Vanderbilt, V. C. (1989). Polarized light angle reflectance instrument. I. Polarized incidence. *Soc. Photo Opt. Inst. Eng.* **1166**, 220-230.

Shashar, N., Cronin, T. W., Wolff, L. B. and Condon, M. A. (1998). The polarization of light in a tropical rain forest. *Biotropica* **30**, 275-285.

Shul'gin, I. A. and Moldau, K. A. (1964). On coefficients of brightness of leaves in nature and polarized light (English translation). *Dokl. Akad. Nauk. SSR Bot. Sci. Sect.* **162**, 99-101.

Speck, M. and Labhart, T. (2001). Carotinoid deprivation and rhodopsin alignment in R1-6 photoreceptors of *Drosophila melanogaster*. In *Proceedings of the 28th Göttingen Neurobiology Conference* (ed. N. Elsner and G. W. Kreutzberg), pp. 514. Stuttgart: Thieme.

Vanderbilt, V. C. and Grant, L. (1985a). Polarization photometer to measure bidirection reflectance factor R(55°, 0°, 55°, 180°) of leaves. *Opt. Eng.* **25**, 566-571.

Vanderbilt, V. C. and Grant, L. (1985b). Plant canopy specular reflectance model. *Inst. Electric. Elect. Eng. Trans. Geosci. Remote Sens.* **23**, 722-730.

Vanderbilt, V. C., Grant, L. and Daughtry, C. S. T. (1985a) Polarization of light scattered by vegetation. *Proc. Inst. Electric. Electron. Eng.* **73**, 1012-1024.

Vanderbilt, V. C., Grant, L., Biehl, L. L. and Robinson, B. F. (1985b) Specular, diffuse and polarized light scattered by wheat canopies. *Appl. Opt.* **24**, 2408-2418.

von Frisch, K. (1965). *Tanzsprache und Orientierung der Bienen*. Berlin: Springer.

Wehner, R. and Bernard, G. D. (1993) Photoreceptor twist: a solution to the false colour problem. *Proc. Natl. Acad. Sci. USA* **90**, 4132-4135.

Wehner, R., Bernard, G. D. and Geiger, E. (1975) Twisted and non-twisted rhabdoms and their significance for polarization detection in the bee. *J. Comp. Physiol.* **104**, 225-245.

Wehner, R. and Strasser, S. (1985). The POL area of the honey bee's eye: behavioural evidence. *Physiol. Entomol.* **10**, 337-349.